Original Article

Institution of MECHANICAL ENGINEERS

Journal of ENGINEERING IN MEDICINE

Proc IMechE Part H:
J Engineering in Medicine
227(7) 746–756

DOI: 10.1177/0954411913483259
pih.sagepub.com
SAGE

Evaluation of a new approach for modelling the screw–bone interface in a locking plate fixation: A corroboration study

Mehran Moazen[1,2], Jonathan H Mak[1], Alison C Jones[1], Zhongmin Jin[1,3], Ruth K Wilcox[1] and Eleftherios Tsiridis[4,5,6]

Abstract

Computational modelling of the screw–bone interface in fracture fixation constructs is challenging. While incorporating screw threads would be a more realistic representation of the physics, this approach can be computationally expensive. Several studies have instead suppressed the threads and modelled the screw shaft with fixed conditions assumed at the screw–bone interface. This study assessed the sensitivity of the computational results to modelling approaches at the screw–bone interface. A new approach for modelling this interface was proposed, and it was tested on two locking screw designs in a diaphyseal bridge plating configuration. Computational models of locked plating and far cortical locking constructs were generated and compared to in vitro models described in prior literature to corroborate the outcomes. The new approach led to closer agreement between the computational and the experimental stiffness data, while the fixed approach led to overestimation of the stiffness predictions. Using the new approach, the pattern of load distribution and the magnitude of the axial forces, experienced by each screw, were compared between the locked plating and far cortical locking constructs. The computational models suggested that under more severe loading conditions, far cortical locking screws might be under higher risk of screw pull-out than the locking screws. The proposed approach for modelling the screw–bone interface can be applied to any fixation involved application of screws.

Keywords

Finite element method, screw–bone interface, fracture fixation, screw pull-out, construct stiffness, locking screw, spring

Date received: 13 November 2012; accepted: 21 February 2013

Introduction

Clinical failure of bone fracture fixation constructs is not common but still occurs.[1–4] This has generated interest from both the biomechanics and orthopaedic trauma communities to investigate the strength and stability of fracture fixation constructs.[3–13] There are several failure mechanisms of these constructs, such as plate failure, screw shaft bending, screw breakage or screw pull-out.[1–3] Screw pull-out, although not common, can occur in cases of poor bone quality,[14] periprosthetic fracture fixations where the presence of a prosthesis may necessitate the use of unicortical screws or where non-locking screws are used. Therefore, a number of studies have been carried out to investigate various design features of screws.[11,13–16] Experimental pull-out tests on a single screw in cadaveric or synthetic bones have been widely used to find out the optimum screw design.[17–20] Such tests provide invaluable information on the performance of a single screw; however, our understanding of the pattern and magnitude of the

[1]Institute of Medical and Biological Engineering, University of Leeds, Leeds, UK
[2]School of Engineering, University of Hull, Hull, UK
[3]State Key Laboratory for Manufacturing System Engineering, School of Mechanical Engineering, Xi'an Jiaotong University, Xi'an, P.R. of China
[4]Academic Department of Orthopaedic and Trauma, University of Leeds, Leeds, UK
[5]Division of Surgery, Department of Surgery and Cancer, Imperial College London, London, UK
[6]Academic Orthopaedics and Trauma Unit, Aristotle University Medical School, Thessaloniki, Greece

Corresponding author:
Mehran Moazen, School of Engineering, University of Hull, Hull HU6 7RX, UK.
Email: Mehran_Moazen@yahoo.com; M.Moazen@hull.ac.uk

load distribution between screws in a fracture fixation construct is still limited.[21]

Computational models based on the finite element (FE) method have potential to assess the performance of screws in fracture fixation constructs. One of the challenges in modelling these constructs arises from defining the screw–bone interfaces. While incorporating screw threads would be a more realistic representation of the physics,[18,20,22–24] this approach can lead to models that are computationally expensive to solve due to the high mesh densities required when a number of screws are used. Several authors have instead suppressed the threads and modelled the screw shaft with fixed conditions assumed at the screw–bone (or cylinder–bone) interface,[25–27] which is referred to here as the 'fixed' condition. However, this approach can lead to an overestimation of the construct stiffness, and it is difficult to estimate the magnitude of the pull-out forces that are experienced by each screw in the construct. Understanding the axial screw forces can potentially shed light on rationale behind the clinical screw pull-out cases[1–3] and facilitate advances to overcome these challenges.

Therefore, the aims of this study were to (1) assess the sensitivity of the computational results to modelling approaches at the screw–bone interface, (2) propose and test a new approach for modelling the screw–bone interface and (3) implement the new approach to estimate the pattern of load distribution and the magnitude of the forces that are experienced by each screw, between two locking screw designs, in a diaphyseal bridge plating configuration. It should also be noted that the computational models were developed based on in vitro study of Bottlang et al.[11] and corroborated against their results in this study. To ensure like-for-like comparison between the computational models in this study and the previously reported experimental models,[11] the authors were contacted and they kindly provided us with all necessary information for this study.

Materials and methods

In the first step, FE models of locked plating (LP) constructs were developed in a diaphyseal bridge plating configuration (Figure 1). Various sensitivity tests were performed (Figure 2) to understand the effect of modelling the screw–bone interface and associated input parameters on the overall stiffness of this construct. Here, a new approach for modelling the screw–bone interface was proposed. In the second step, FE models of far cortical locking (FCL) constructs were developed based on the parameters that best fitted the experimental data of the LP case. The models were assembled to correspond to the experimental tests of Bottlang et al.[11] on synthetic femoral diaphysis bone and were loaded under same magnitude and loading conditions (i.e. axial compression, torsion and bending).

Model development

Computer-aided design (CAD) models of the locking plate and the locking and FCL screws were provided by Bottlang et al.[11] as described in their study. In brief, the plate had 11 holes, a thickness of 4.5 mm, a width of 17.5 mm and a length of 200 mm. The locking screws had a uniform outer diameter of 4.5 mm and a core diameter of 4 mm. The far locking screws had a section with a diameter of 3.2 mm, to avoid any fixation at the near cortex, and an outer diameter of 4.5 mm at the far cortex (Figure 1). To assess sensitivity of the FE results to the diameter of the modelled screws, locking screws were modelled with 4 and 5 mm diameters (sensitivity 2 in Figure 2). FCL screws were modelled with a 4 mm diameter (core diameter) at the far cortex. In all cases, screw threads were suppressed (Figure 1).

These implants were used to fix a transverse fracture, with a 10 mm fracture gap, in a cylindrical model replicating a non-osteoporotic femoral diaphysis with an outer diameter of 27 mm and a wall thickness of 7 mm.[11] The modelled diaphysis is analogous to the medium-size fourth-generation composite Sawbones femur (#3403; Pacific Research Laboratories, Vashon, WA, USA). For each plating case, screws were placed in the first, third and fifth holes from the fracture site (Figure 1). The far locking screw fixations were arranged in a staggered 9° angle configuration (Figure 1). This configuration was used in the experimental study[11] to increase the torsional stiffness of the FCL construct. The two construct fixations were assembled with a 1 mm gap between the plate and bone in SolidWorks (Dassault Systèmes SolidWorks Corp., Concord, MA, USA). These models were then exported to a FE package (ABAQUS v. 6.9; Simulia Inc., Providence, RI, USA).

Material properties

All sections were assigned isotropic material properties with an elastic modulus of 16.3 GPa for the synthetic bone[28] and 110 GPa for the titanium plate and screws.[27] Poisson's ratio of 0.3 was used for all materials.[27] These properties were chosen to match the study of Bottlang et al.[11]

Interactions

The interface between the screw head and plate was fixed. Penalty-based contact conditions were specified at both the plate–bone interface and between the mid-shaft of the FCL screws and the bone at the near cortex with a coefficient of friction of 0.37[29] and normal contact stiffness of 600 N/mm.[30] It should be noted that plate–bone contact was not found to occur under the loading considered in this study.

Two approaches were tested for modelling the screw–bone interface in the locking constructs (sensitivity 1 in Figure 2): one where all relative movement was

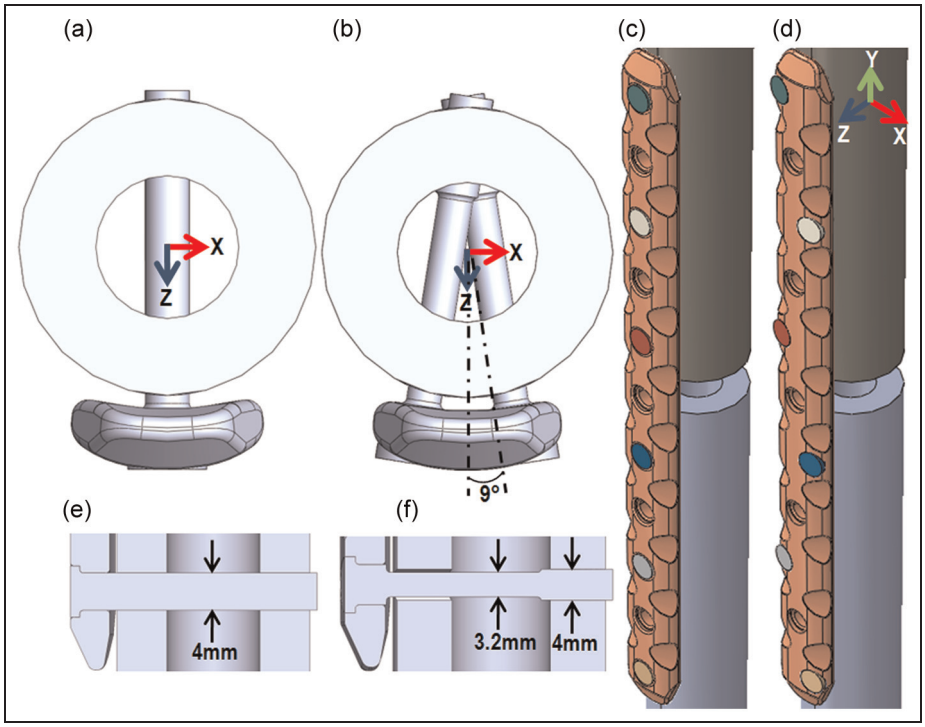

Figure 1. (a) and (b) the locked plating and far cortical locking constructs from dorsal view; (c) and (d) the locked plating and far cortical locking constructs in isometric view; (e) and (f) the cross-sectional view of screw–bone interface from the most distal screw.

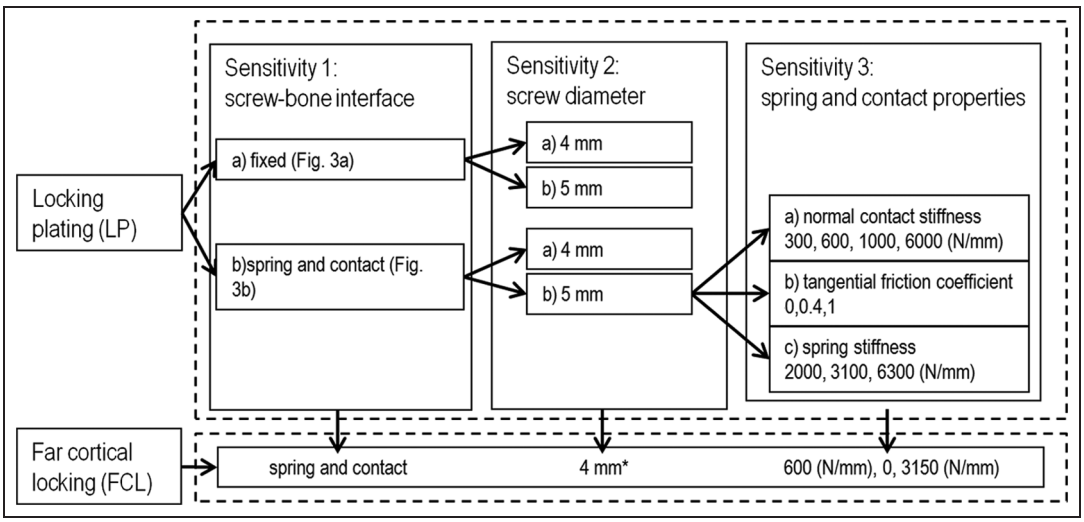

Figure 2. A schematic of this study.
*FCL screws had midshaft diameter of 3.2 mm with 4 mm diameter at the far cortex.

prevented ('fixed') and one allowing micromovement at these interfaces ('spring and contact'). Both approaches are illustrated in Figure 3. The latter approach was implemented using spring and contact elements. Here, sliding contact conditions were created between the screw and the bone, while screw pull-out/push-in was resisted by attaching two spring elements between the screw and the bone (as it is shown in Figure 3), allowing some relative movement at this interface. The spring elements spanned the length of screw where the thread would be embedded into bone, with the far cortex end attached to the screw and the near cortex end attached to the bone. It should be noted that (1) the spring attachment point on the bone for LP was on the near cortex and for the FCL was on the far cortex; (2) the spring forces were independent of the initial lengths (i.e. $F = K \times dL$, where F is the force, K is the spring stiffness and dL is the difference between the spring length before and after loading); (3) any number of spring elements could have been chosen; however, since these are effectively attached in parallel to each other, the stiffness of each spring should be equal to the total stiffness

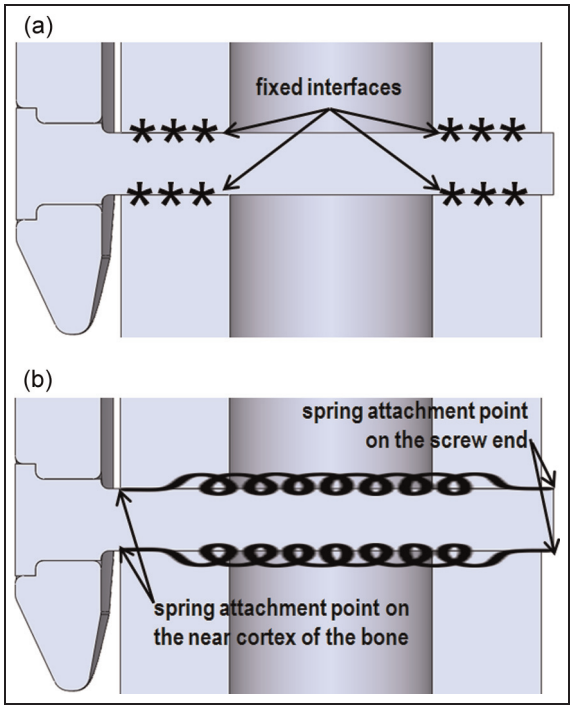

Figure 3. Schematic of screw–bone interface modelling approaches: (a) fixed condition and (b) spring and contact elements at the screw–bone interface. Note that in (b), each spring connects the end of the screw to the cortical bone under the plate.

divided by the number of springs. This approach required further assumptions in relation to the choice of contact and total spring stiffness parameters. Therefore, further sensitivity tests were performed.

Contact was modelled using a penalty-based contact condition with a frictionless coefficient and a normal contact stiffness. A frictionless contact was used since the spring elements constrained the transverse motion at the screw–bone interface. The normal contact stiffness was initially set to 600 N/mm based on the study by Bernakiewicz and Viceconti[30] who found that this value for the titanium–bone interface closely replicated the subsidence of a cementless hip stem. This contact stiffness value was then altered to 300, 1000 and 6000 N/mm[31] for sensitivity test 3a. The value of 600 N/mm was used as the baseline value since it led to a closer match to the axial stiffness experimental results; torsional and bending rigidities showed minimal sensitivity to this parameter. The friction coefficient was altered to 0.4 and 1 for sensitivity test 3b to cover the range of experimental data reported in literature[32,33] (Figure 2). As a baseline value, springs were modelled with stiffness based on screw pull-out test of Zdero et al.[19] This group reported an average ultimate pull-out force and work to pull-out of 6390 N and 6.5 J, respectively, for 4.5 mm screws on femoral diaphysis with similar mechanical properties to those used in this study. Based on these values, an elastic screw displacement of 2.034 mm was calculated (i.e. (2 × work)/load = displacement − (2 × 6.5 J)/6390 N = 2.034 mm), and based on this displacement, a total stiffness of 3141 N/mm (i.e. load/displacement = stiffness − 6390 N/2.034 mm = 3141 N/mm) was calculated for both springs for the initial elastic pull-out of the screw. The total spring stiffness was altered to 2000 and 6300 N/mm for sensitivity test 3c (Figure 2); the tested range covered the experimental pull-out results reported in the literature.[19] Note that any radial pre-stress at the screw–bone interface due to the screw insertion was not considered in this study.

In all cases, stiffness values were compared under three loading conditions (as described in section 'Boundary conditions and loads'). The baseline values were used for all FCL models, except spring stiffness where the baseline value was halved, as screws are initially in contact with bone at just far cortex.[19]

Boundary conditions and loads

The constructs were loaded under three loading conditions. Axial compression of 1 kN and torsion of 10 N m were applied separately to the proximal end of the bone. Here, a node was created at the centre of the most proximal section of the bone, and it was coupled with the surface area of the bone. This node was constrained under axial loading in *X*- and *Z*-axes while it was free to rotate in all directions; under torsion, all its degrees of freedom were constrained except rotation around *Y*-axis. The distal end was rigidly fixed. Four-point bending (around the *X*-axis –Figure 1) was modelled with the upper and lower supports separated by 290 and 400 mm, respectively,[11] while the construct was loaded to generate constant bending of 10 N m across the plate. Here, the bone was constrained at the support point only along *Z*-axis (see Figure 1 for *X*-, *Y*- and *Z*-axes). The aforementioned boundary conditions were applied to replicate the experimental set-up.

Mesh sensitivity

Tetrahedral (C3D10M) elements were used to mesh all the components in a FE package (ABAQUS v. 6.9; Simulia Inc.). Convergence was tested by increasing the number of elements from 70,000 to 1,600,000 in five steps. The solution converged on the parameter of interest ($\leqslant$5% – axial stiffness, torsional and bending rigidities as well as spring force) with approximately 400,000 elements. The spring forces converged at an element size of approximately 0.5 mm at the screw–bone interface.

Simulations and measurements

The models were solved and analysed in ABAQUS. The axial stiffness was calculated by dividing the magnitude of axial load by displacement of the proximal section of the specimens. Torsional stiffness was calculated by dividing the magnitude of torsion by the rotation around the diaphyseal axis. Torsional stiffness was

Table 1. Sensitivity of the overall stiffness of locked plating construct to the screw–bone interface modelling approaches and screw diameter. Sensitivity results are also compared to the experimental results of Bottlang et al.[11]

Locked plating	Computational (this study)				Experimental[11]
	Fixed		Spring and contact		
Screw diameter (mm)	4	5	4	5	4.5
Axial stiffness (kN/mm)	5.3	7.0	3	3.8	2.9 ± 0.13
Torsional rigidity (N m^2/deg)	0.98	1.27	0.60	0.87	0.4 ± 0.03
Bending rigidity (N m^2)	86.2	89.1	61.7	69.2	82.9 ± 1.96

Experimental values are reported as the mean and the standard deviation.

multiplied by the specimen length of 260 mm to derive torsional rigidity. Bending stiffness was expressed in terms of flexural rigidity as $EI = Fa^2 \times (3l - 4a)/12y$, where F is the total applied force, l is the distance between the lower supports (400 mm), a is the distance between the lower and upper supports (55 mm) and y is the displacement of the diaphysis at the applied load.[11] Interfragmentary motion was quantified at the near and far cortices of the bone by determining the relative displacements in the frontal plane between the most distal point of the proximal fragment and the most proximal point of the distal fragment.

Results

Increasing the screw diameters by 1 mm (25%) led to an increase in axial stiffness and torsional and bending rigidities of the construct of 32%, 30% and 3%, respectively (Table 1 – fixed condition). A similar pattern of stiffness increase was found when increasing the diameter with the alternative screw–bone interface condition (Table 1 – spring and contact). Moving from the fixed to the spring and contact interface condition caused a reduction in axial stiffness and torsional and bending rigidities of the construct by 44%, 39% and 28%, respectively, based on the 4 mm screw diameter (Table 1).

Sensitivity tests on the input parameters for the spring and contact approach (with screw diameter of 5 mm) showed that increasing the normal contact stiffness, friction coefficient and spring stiffness each led to an increase in the axial stiffness and torsional and bending rigidities of construct (Table 2). Over the range of tested input parameters, axial stiffness and torsional rigidity were most sensitive to the normal contact stiffness (a maximum increase of 50% and 17%) followed by the friction coefficient (maximum increase of 17% and 8%) and spring stiffness (maximum increase of 5% and 0%). Bending rigidity was most sensitive to the friction coefficient followed by spring stiffness and normal contact stiffness (7%, 6% and 6%, respectively).

The load–displacement behaviour of LP and FCL constructs are compared in Figure 4, for both previous experimental tests and the current computational models (using the spring and contact approach). The models successfully replicated the experimental bilinear

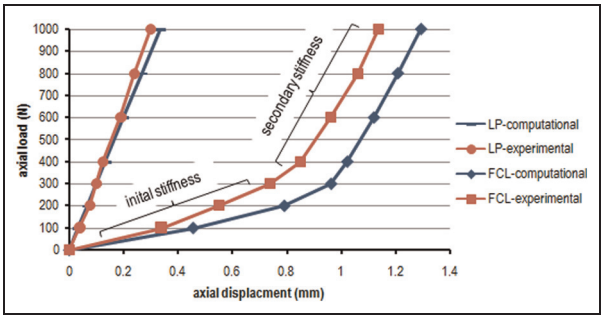

Figure 4. A comparison between the axial stiffness of LP and FCL constructs based on the computational (this study) and experimental[11] results. Note that FCL constructs showed an initial and secondary stiffness (bilinear stiffness or progressive stiffening). These results were obtained with a screw diameter of 4 mm.
LP: locked plating; FCL: far cortical locking.

stiffness in the FCL case, with a predicted initial stiffness of 0.29 kN/mm and a secondary stiffness of 2.3 kN/mm (for a load >400 N). The initial stiffness of this construct was 90% lower than LP stiffness (3 kN/mm based on computational model).

Equivalent bilinear behaviour of the FCL was predicted under torsion, with a rigidity of 0.11 N m^2/deg initially, followed by a secondary rigidity of 0.41 N m^2/deg with a torsion >1 N m. Here, the FCL initial rigidity was 82% lower than the LP construct (0.6 N m^2/deg). In bending, the computational model did not predict a bilinear rigidity, yet it showed 13% reduction in rigidity compared to the LP (61.7 N m^2– see Table 3).

A comparison of interfragmentary motion between the LP and FCL construct types, under 200 N axial load, is shown in Figure 5. The LP construct showed less than 0.2 mm of movement at both cortices. Although the FCL construct showed more movement than the LP case, it remained less than 1 mm. The near cortex to far cortex interfragmentary motion ratios for the LP and FCL constructs were 0.4 and 0.92, respectively (Figure 5).

High levels of von Mises stress were observed under the considered loading conditions at similar positions to the points of failures in the experimental study. A qualitative comparison of the von Mises stress across the models is shown in Figure 6; here, dashed lines

Table 2. Sensitivity of the overall stiffness of locked plating construct to the input parameters used in the spring and contact approach for modelling the screw–bone interface.

	Normal contact stiffness (N/mm)					% of maximum increase	Tangential friction coefficient			% of maximum increase	Spring stiffness (N/mm)			% of maximum increase
	300	600[a]	1000	6000	1900		0[a]	0.4	1	–	2000	3100[a]	6300	215
Axial stiffness (kN/mm)	3.2	3.8	4.1	4.8	50		3.8	4.1	4.4	17	3.7	3.8	3.9	5
Torsional rigidity (N m^2/deg)	0.82	0.87	0.90	0.96	17		0.87	0.91	0.93	8	0.87	0.87	0.87	0
Bending rigidity (N m^2)	68.1	69.1	69.9	72.5	6		69.1	71.8	74.3	7	67.3	69.1	71.2	6

[a] The baseline values for the sensitivity tests.
The results were obtained with screw diameter of 5 mm.

highlight the experimental failure zone. Under axial loading, the bone in the experimental model failed around the most distal screw[11] in a pattern comparable to the region of high level of stress that the computational model predicted. Under torsion, the LP screws failed at the plate–bone interface and FCL screws were bent; in both cases, elevated levels of von Mises stress were found in the screws. Under bending, bone failure occurred experimentally at either most proximal or most distal screw where also computationally a high level of stress was observed.

The spring forces, which represent the forces acting in the direction of the screw shafts, are shown in Figure 7 for the LP and FCL constructs. Under axial loading of 200 and 1000 N, the closest screw to the fracture side on the distal fragment (S4 in Figure 7) experienced the highest spring force. Comparing the LP and FCL constructs at this screw, the FCL showed 92% (under 200 N) and 25% (under 1000 N) increase in the total spring forces. Under torsion, the spring forces in the FCL construct were considerably higher than in the LP construct. For instance, under torsion of 1 and 10 N m at the screw number 4 (S4 – see Figure 7), the total spring forces for the FCL construct compared to the LP construct were over a hundred times (18.17 vs 0.17 N) and seven times (113.17 vs 15.21 N) higher, respectively.

Discussion

Computational models of LP and FCL constructs were developed based on in vitro models of Bottlang et al.[11] Corroboration with experimental data was undertaken to build confidence in the results of the computational models.[34,35] The general trends of experimental stiffness and fracture movement were replicated computationally. The computational models were used to investigate (1) the sensitivity of the FE results to modelling approaches at the screw–bone interface and (2) the pattern of load distribution between the screws in the LP and FCL constructs.

Sensitivity tests highlighted that modelling the screw–bone interface with the new proposed approach, and with cylindrical screws that matched the core diameter of the experimental screws, generally led to a closer agreement between the overall stiffness of the computational and experimental models in the LP construct. Therefore, the same conditions were used in modelling the FCL construct. These results also highlighted that 'fixed' modelling of the interfaces in computational models underestimated the potential screw–bone micromovements that are present in reality during elastic deformation and therefore led to an overestimation of the overall construct stiffness, for example, by 83% based on screw diameter of 4 mm for axial stiffness (Table 1). Such overestimation can vary depending on the applied loading to the system. Comparing the two approaches that were tested for modelling the screw–bone interface with a model

Table 3. A comparison between the overall stiffness of LP and FCL constructs based on the computational and experimental[11] models.

	Computational (this study)			Experimental[11]		
	LP	FCL	%reduction	LP	FCL	%reduction
Axial stiffness (kN/mm)	3.0	0.29/2.29	90	2.9 ± 0.13	0.36 ± 0.05/2.26 ± 0.08	88
Torsional rigidity (N m^2/deg)	0.6	0.11/0.41	82	0.4 ± 0.03	0.17 ± 0.04/0.32 ± 0.01	57
Bending rigidity (N m^2)	61.7	53.4	13	82.9 ± 1.96	59 ± 1.3/68.1 ± 3.3	29

LP: locked plating; FCL: far cortical locking.
Experimental values were given as the mean and the standard deviation; %reduction was calculated based on the initial stiffness of the FCL constructs.

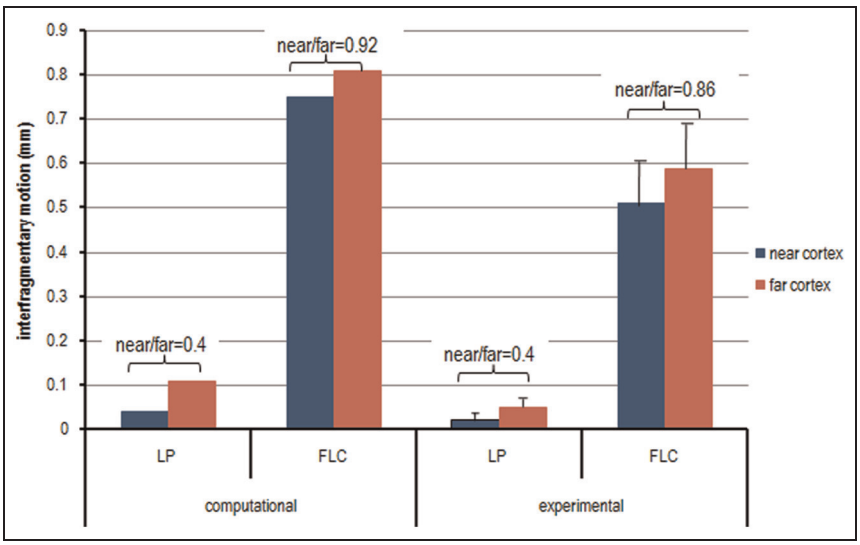

Figure 5. Comparison of the interfragmentary motion between the computational and experimental[11] models in LP and FCL constructs on the near and far cortices. Results obtained under axial loading of 200 N and for experiments are reported as the mean and the standard deviation.
LP: locked plating; FCL: far cortical locking.

including the threads was beyond the scope of this study and would require detail modelling of the threads. A recent study by MacLeod et al.[36] found that in a model where threads were included, modelling the screw–bone interface with contact elements or 'fixed' condition led to similar predictions of the overall stiffness. However, they did not compare their results against any experimental data. Therefore, it is likely that modelling the threads in this study with the parameters used by MacLeod et al.[36] would have generated results similar to the 'fixed' interface condition. Nevertheless, once threads are included in the model, still the interface conditions need to be determined and there would be parameters such as friction coefficient and normal contact stiffness to derive.

The results of the spring and contact sensitivity tests in the LP construct showed that axial stiffness and torsional rigidity were most sensitive to the normal contact stiffness. In solving the contact problem at each contact pair, overclosure is monitored at nodes and must be corrected at the contact surface. The magnitude of the required push back force is calculated based on the overclosure through a contact stiffness matrix.[30] Contact stiffness depends on the shape, size and material properties of the construct and does not have any physical meaning.[30] Higher values of contact stiffness can lead to an ill-conditioned numerical problem (over constraint issues and a higher number of iterations), while a low contact stiffness produces higher overclosure and contributes some degree of stress inaccuracy.[30,37] This explains the sensitivity to contact stiffness of the presented results under axial load and torsion, which perhaps led to a greater degree of overclosure at the screw–bone interface. Under bending, the results were much less sensitive to the contact stiffness and more sensitive to the friction coefficient and spring stiffness (Table 2), which constrain the longitudinal movement of the screws. This added to the fact that fixed conditions (Table 1) led to closer agreement between the computational and experimental models under bending (86.2 vs 82.9 N m^2, respectively) suggest that the screw–bone interface under bending was under high longitudinal force and perhaps minimal radial overclosure.

Since the spring–contact approach generally fitted more closely to the experimental results,[11] in the LP

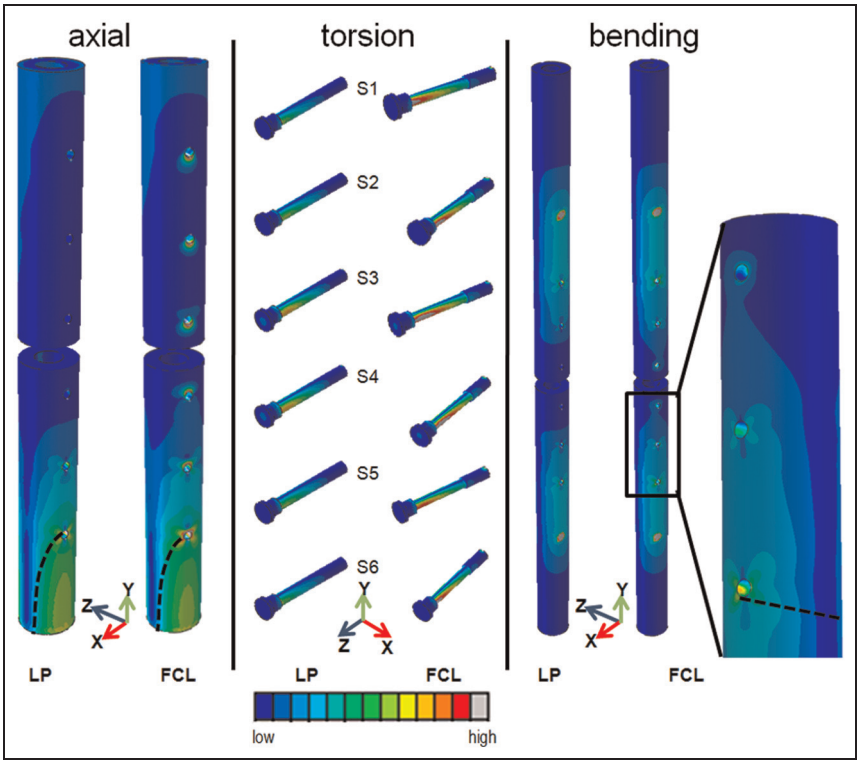

Figure 6. Von Mises stress distribution. In the experimental models,[11] under torsion, LP construct failed due to screw breakage at the plate–bone interface and FCL construct failed due to screw bending.
LP: locked plating; FCL: far cortical locking.
Dashed lines highlight the experimental failure zone.

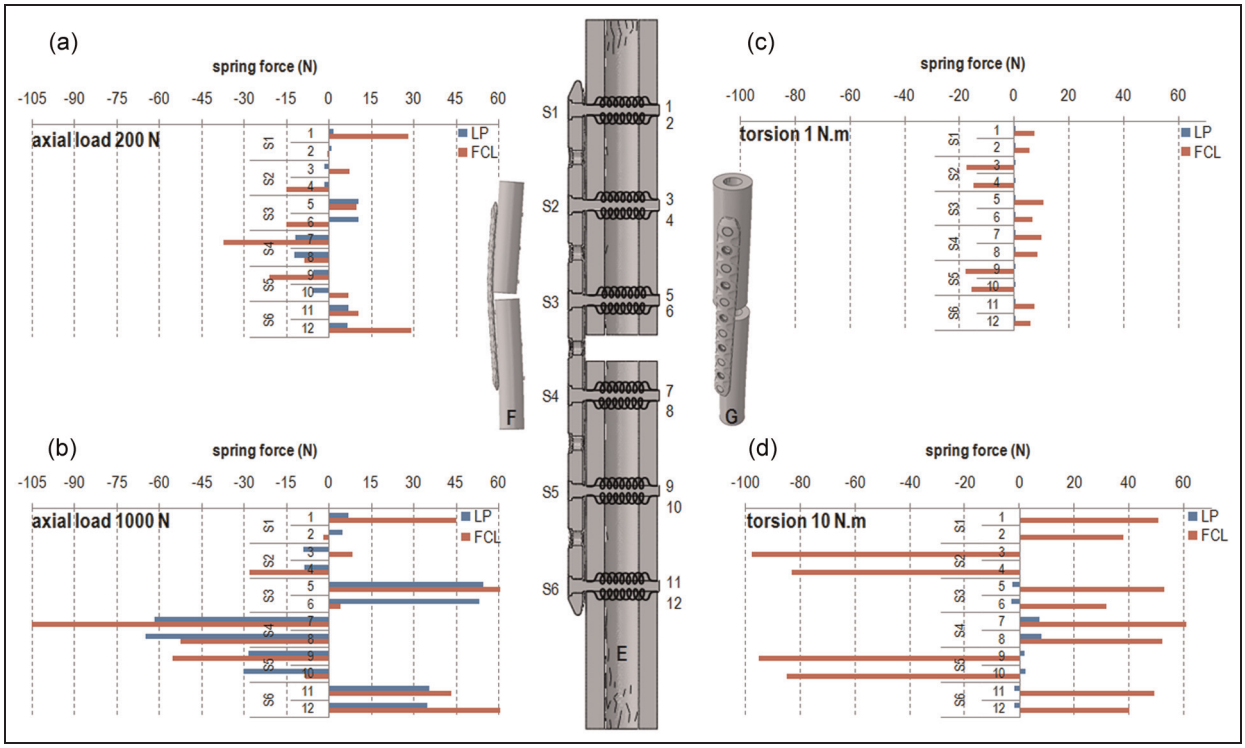

Figure 7. Comparison of the spring forces between the LP and FCL constructs under axial load of (a) 200 N and (b) 1000 N and torsion of (c) 1 N m and (d) 10 N m. Positive values indicate push-in and negative values indicate pull-out. (e) The cross-section of the construct along the *X*-axis. (f) and (g) Deflection of the LP construct under axial loading of 1000 N and torsion of 10 N m.
LP: locked plating; FCL: far cortical locking.
Deflections are magnified 10 times.

construct, it was expected that a close agreement between the computational and experimental data in the FCL construct should be obtained. Also of interest was whether the new approach was capable of predicting the experimental differences between the two screw designs, in terms of stiffness and interfragmentary motion.

The computational model using the new approach predicted a bilinear axial stiffness behaviour, which was experimentally reported for the FCL construct (Figure 4). Comparing the initial stiffness of the FCL (0.29 kN/mm) with the LP (3 kN/mm) construct showed a 90% reduction in the former construct. This was comparable to the 88% reduction found experimentally (see Table 3). Although there were differences between the computational and experimental displacement data under axial loading in the FCL construct (Figure 4), a comparable pattern of torsional rigidity between the computational and experimental results was found. However, under bending, the computational models using the spring and contact approach (with baseline parameter values) were unable to predict the bilinear stiffness that was found experimentally for the FCL construct because the screw shaft did not come in contact with the near cortex. In fact, the new approach also underestimated the bending rigidity of the LP construct by 25% (see Table 3). But it should be noted that the experimental models showed an almost linear stiffness under bending with 15% difference between the initial and secondary stiffness in the FCL construct (59 and 68.1 N m^2, respectively). In terms of interfragmentary motion results, while there were differences (up to 47%) between the computational and experimental results, it was interesting that the near cortex to far cortex interfragmentary motion ratios for the LP and FCL for the computational and experimental models were almost the same (see Figure 5). The discrepancies between the results of experimental and computational models could be due to minor differences in, for example, the loading apparatus, material properties or measurement position (in the case of interfragmentary motion).

Despite the discrepancy between the computational and experimental models, both models captured the reduction in stiffness of FCL in comparison to the LP construct. Furthermore, computational models of both LP and FCL constructs qualitatively predicted high level of stress in the locations where experimental models failed. This provides confidence in the computational models despite the numerical discrepancies with the experimental models. It should be noted that since experimental strain measurement was not performed in the original experiments by Bottlang et al.,[11] it was not possible to directly corroborate the computational strain predictions, so only a qualitative contour plot of von Mises stress was presented in Figure 6.

The approach developed in this study to model the screw–bone interface (i.e. using spring and contact elements) allows us to, first, incorporate the elastic deformation that occurs at the screw–bone interface into the computational models that seems to better replicate the in vitro experimental model albeit considering that spring stiffness is based on experimental pull-out data. Second, it also estimates the axial resistive force between the screw and the bone from the spring forces. By predicting the forces that screws are experiencing in fracture fixation constructs, the performance of the screws can be optimized to reduce the risk of pull-out.[22] Future studies need to be undertaken in this respect to find the optimum screw design in the case of poor bone quality[14] or periprosthetic fracture fixations[1,2,38] where there is higher risk of screw pull-out, and it is likely that the predicted axial screw forces would be increased compared to this study. In this study, the capability of the presented approach was shown in comparing the screw forces experienced by two different screw designs.

The difference in the total spring forces between the LP and FCL constructs was higher during the initial loading, corresponding to the initial stiffness, than during the secondary loading, for example, 92% versus 25% for S4 at 200 and 1000 N axial load, respectively. Also, there was a higher difference between the forces of two springs in each screw in the FCL construct compared to the LP construct, for example, 77% versus 4% for S4 at 200 N, respectively. Both aforementioned differences are due to the underlying design behind FCL screws that provide far cortical fixation (one cortex fixation) during the initial loading and that (1) progressively stiffen the construct as the screws come into contact with the bone at the near cortex[11] and (2) undergo higher bending comparing to the locking screw (across X-axis as shown in Figure 1) that is captured in the differences between the forces of two springs (see Figure 7). Nevertheless, the spring forces were higher in the case of FCL compared to the LP constructs, suggesting that under more severe loading conditions, FCL screws might be under higher risk of screw pull-out than the locking screws. However, under axial loading of 200 N that corresponds to the toe-touch weight bearing recommended for the immediate postoperative period,[39] the maximum spring forces of approximately −24 and −46 N (note negative values indicate pull-out) were predicted at screw number 4 (S4) for LP and FCL constructs (Figure 7(a)). The aforementioned spring forces are considerably lower than the ultimate pull-out force values reported by Zdero et al.[19] for a 4.5 mm screw on femoral diaphysis with similar mechanical properties to those used in this study (i.e. 6390 N for bicortical screws). Nevertheless, care must be taken in using the spring forces reported here as these are clearly dictated by the spring stiffness values and the boundary conditions used in this study. Inexact modelling of these input parameters could lead to unrealistic transverse motion at the screw–bone interface. Estimating screw loosening under cyclic loading based on spring forces predicted in this study would be possible, but it would require further experimental data on cyclic loading of single screw pull-out.

There are a number of limitations in both experimental and computational models considered in this study. Perhaps the most significant are the following: (1) an idealized diaphyseal shaft was modelled where rigid distal fixation was assumed and effect of muscle forces was eliminated – these are likely to alter the loading condition applied to the construct – addition of the muscle forces would minimize the bending moments and lead to axial loading of the bone; these can potentially increase the predicted stiffness values[40] and reduce the predicted spring forces presented in Figure 7. (2) An unrealistic fracture gap was used – orthopaedic surgeons aim to completely reduce the fracture gap, which would lead to an overall more mechanically stable construct, yet perfect fracture reduction is challenging. (3) The assigned material properties were those of synthetic bone fixed with a plate and screws made of titanium. A less stiff bone would reduce the overall stiffness values predicted in this study[11] and is likely to increase the chance of screw pull-out. A stiffer plate and screw material, such as stainless steel, are likely to increase stiffness predictions and they would perhaps reduce the chance of screw pull-out (considering the unrealistic fracture gap) and mechanical failure. (4) Static loading was considered – where in reality, the fracture fixation construct is under cyclic loading and loss of system stiffness and fatigue failure can be an issue. However, perhaps as far as partial load bearing is applied, callus formation can occur[41] that will reduce the fixation load bearing; further investigations in this regard are required. Furthermore, in the computational models, the screw insertion torque was not modelled. Insertion torque creates radial pre-stress that has local effect on the bone at the screw–bone interface but likely minimal effect on the overall construct stiffness of locking plates. In this study, computational models using different approaches of screw–bone modelling were capable of replicating the experimental models with less than 5% difference under axial loading and bending without including such pre-stress. However, under torsion, larger differences between the computational and experimental models were observed where the lack of radial pre-stress at the screw–bone interface could have been a contributing factor. Nevertheless, the assumptions made in this study were kept the same for both the LP and FCL constructs (in both the current computational and the referenced experimental models) to ensure that the comparison between the constructs remains valid and this is where the emphasis through this study was placed.

Conclusion

This article described development of a computational model of LP and FCL constructs in a diaphyseal bridge plating configuration based on the experimental tests of Bottlang et al.[11] Several sensitivity analyses were performed on the aspects of modelling approaches at the screw–bone interface. A new approach for modelling the screw–bone interface was proposed and tested. The results highlighted that representing the screw–bone interface as a 'fixed' condition led to an overestimation of the overall construct stiffness. The proposed approach with 'spring and contact' elements led to closer agreement with the experimental stiffness data. Using the proposed approach, the pattern of load distribution and the magnitude of the axial forces that were experienced by each screw were estimated between the LP and FCL constructs. These models also showed that FCL screws might be under higher risk of pull-out compared to the locking screws under more severe loading conditions. The proposed approach for modelling the screw–bone behaviour can be applied to any fixation that involved application of screws.

Funding

This work is supported by British Orthopaedic Association (BOA) through the Latta Fellowship and was partially funded through WELMEC (Wellcome Trust and EPSRC under grant WT 088908/Z/09/Z) and LMBRU through National Institute for Health Research (NIHR).

Acknowledgements

We would like to thank Dr Bottlang and Dr Feist for provision of the technical drawings for FCL constructs and for their guidance in FEA development.

Declaration of conflicting interests

The authors confirm that there is no conflict of interest in this article.

Ethical approval

Not required.

References

1. Tsiridis E, Narvani AA, Timperley JA, et al. Dynamic compression plates for Vancouver type B periprosthetic femoral fractures: a 3-year follow-up of 18 cases. *Acta Orthop* 2005; 76: 531–537.
2. Buttaro MA, Farfalli G, Paredes Nunez M, et al. Locking compression plate fixation of Vancouver type-B1 periprosthetic femoral fractures. *J Bone Joint Surg Am* 2007; 89: 1964–1969.
3. Gardner MJ, Evans JM and Dunbar RP. Failure of fracture plate fixation. *J Am Acad Orthop Surg* 2009; 17: 647–657.
4. Hak DJ, Toker S, Yi C, et al. The influence of fracture fixation biomechanics on fracture healing. *Orthopedics* 2010; 33(10): 752–755.
5. Perren SM. Physical and biological aspects of fracture healing with special reference to internal fixation. *Clin Orthop Relat Res* 1979; 138: 175–196.
6. Goodship AE and Kenwright J. The influence of induced micromovement upon the healing of experimental tibial fractures. *J Bone Joint Surg Br* 1985; 67: 250–255.

7. Wolf S, Janousek A, Pfeil J, et al. The effects of external mechanical stimulation on the healing of diaphyseal osteotomies fixed by flexible external fixation. *Clin Biomech (Bristol, Avon)* 1998; 13: 359–364.
8. Bishop NE, Schneider E and Ito K. An experimental two degrees-of-freedom actuated external fixator for in vivo investigation of fracture healing. *Med Eng Phys* 2003; 25: 335–340.
9. Egol KA, Kubiak EN, Fulkerson E, et al. Biomechanics of locked plates and screws. *J Orthop Trauma* 2004; 18: 488–493.
10. Sun Z, Rafferty KL, Egbert MA, et al. Masticatory mechanics of a mandibular distraction osteogenesis site: interfragmentary micromovement. *Bone* 2007; 41: 188–196.
11. Bottlang M, Doornink J, Fitzpatrick DC, et al. Far cortical locking can reduce stiffness of locked plating constructs while retaining construct strength. *J Bone Joint Surg Am* 2009; 91: 1985–1994.
12. Claes L. Biomechanical principles and mechanobiologic aspects of flexible and locked plating. *J Orthop Trauma* 2011; 25: S4–S7.
13. Moazen M, Jones AC, Leonidou A, et al. Rigid versus flexible plate fixation for periprosthetic femoral fracture – computer modelling of a clinical case. *Med Eng Phys* 2012; 34: 1041–1048.
14. Seebeck J, Goldhahn J, Morlock MM, et al. Mechanical behavior of screws in normal and osteoporotic bone. *Osteoporos Int* 2005; 16(Suppl. 2): 107–111.
15. Perren SM. The concept of biological plating using the limited contact dynamic compression plate (LC-DCP): scientific background, design and application. *Injury* 1991; 22(Suppl. 1): 1–41.
16. Stoffel K, Dieter U, Stachowiak G, et al. Biomechanical testing of the LCP – how can stability in locked internal fixators be controlled? *Injury* 2003; 34(Suppl. 2): B11–B19.
17. DeCoster TA, Heetderks DB, Downey DJ, et al. Optimizing bone screw pullout force. *J Orthop Trauma* 1990; 4: 169–174.
18. Battula S. *Experimental and numerical evaluation of the pullout strength of self-tapping bone screw in normal and osteoporotic bone*. PhD Thesis, University of Akron Press, Akron, OH, 2007.
19. Zdero R, Rose S, Schemitsch EH, et al. Cortical screw pullout strength and effective shear stress in synthetic third generation composite femurs. *J Biomech Eng* 2007; 129(2): 289–293.
20. Feerick EM and McGarry PJ. Cortical bone failure mechanisms during screw pullout. *J Biomech* 2012; 45: 1666–1672.
21. Wieding J, Souffrant R, Fritsche A, et al. Finite element analysis of osteosynthesis screw fixation in the bone stock: an appropriate method for automatic screw modelling. *PLoS One* 2012; 7(3): e33776.
22. Gefen A. Optimizing the biomechanical compatibility of orthopedic screws for bone fracture fixation. *Med Eng Phys* 2002; 24: 337–347.
23. Hou SM, Hsu CC, Wang JL, et al. Mechanical tests and finite element models for bone holding power of tibial locking screws. *Clin Biomech (Bristol, Avon)* 2004; 19: 738–745.
24. Chatzistergos PE, Magnissalis EA and Kourkoulis SK. A parametric study of cylindrical pedicle screw design implications on the pullout performance using an experimentally validated finite-element model. *Med Eng Phys* 2010; 32: 145–154.
25. Ferguson SJ, Wyss UP and Pichora DR. Finite element stress analysis of a hybrid fracture fixation plate. *Med Eng Phys* 1996; 18: 241–250.
26. Shah S, Kim SYR, Dubov A, et al. The biomechanics of plate fixation of periprosthetic femoral fractures near the tip of a total hip implant: cables, screw, or both? *Proc IMechE, Part H: J Engineering in Medicine* 2011; 225: 1–12.
27. Chen G, Schmutz B, Wullschleger M, et al. Computational investigation of mechanical failures of internal plate fixation. *Proc IMechE, Part H: J Engineering in Medicine* 2010; 224: 119–126.
28. Heiner AD. Structural properties of fourth-generation composite femurs and tibias. *J Biomech* 2008; 41: 3282–3284.
29. Hayes WC and Perren SM. Plate-bone friction in the compression fixation of fractures. *Clin Orthop* 1972; 89: 236–240.
30. Bernakiewicz M and Viceconti M. The role of parameter identification in finite element contact analysis with reference to orthopaedic biomechanics applications. *J Biomech* 2002; 35: 61–67.
31. Zhang M, Don X and Fan Y. Stress analysis of osseointegrated transfemoral prosthesis: a finite element model. In: *Conference proceedings of the IEEE engineering in medicine and biology society*, 2005, vol. 4, pp.4060–4063.
32. Shirazi-Adl A, Dammak M and Paiement G. Experimental determination of friction characteristics at the trabecular bone/porous-coated metal interface in cementless implants. *J Biomed Mater Res* 1993; 27(2): 167–175.
33. Cai Z, Zhu M and Yu H. A comparative study on the fretting behaviors of human femur compact bone under tangential and radial fretting models in vitro. In: *International conference on BioMedical Engineering and Informatics*, 2008, vol. 2, pp.310–314.
34. Viceconti M, Olsen S, Nolte LP, et al. Extracting clinically relevant data from finite element simulations. *Clin Biomech (Bristol, Avon)* 2005; 20: 451–454.
35. Anderson AE, Ellis BJ and Weiss JA. Verification, validation, and sensitivity studies in computational biomechanics. *Comput Methods Biomech Biomed Engin* 2007; 10: 171–184.
36. MacLeod AR, Pankaj P and Simpson AHRW. Does screw-bone interface modeling matter in finite element analyses? *J Biomech* 2012; 45: 1712–1716.
37. ABAQUS Inc., *ABAQUS theory manual 6.5*, http://www.abaqus.com
38. Moazen M, Jones AC, Jin Z, et al. Periprosthetic fracture fixation of the femur following total hip arthroplasty: a review of biomechanical testing. *Clin Biomech (Bristol, Avon)* 2011; 26: 13–22.
39. Ruedi T and Leutenegger A. After-care of fractures, especially following osteosynthesis. *Ther Umsch* 1989; 46: 435–440 (in German).
40. Duda GN, Heller M, Albinger J, et al. Influence of muscle forces on femoral strain distribution. *J Biomech* 1998; 31: 841–846.
41. Augat P, Merk J, Ignatius A, et al. Early, full weightbearing with flexible fixation delays fracture healing. *Clin Orthop Relat Res* 1996; 328: 194–202.